KSÜ Mühendislik Bilimleri Dergisi, 29(3), 2026
Araştırma Makalesi

KSU J Eng Sci, 29(3), 2026
Research Article

Kahramanmaras Sutcu Imam University
Journal of Engineering Sciences

Geliş Tarihi : 13.03.2026
Kabul Tarihi : 16.06.2026

Received Date : 13.03.2026
Accepted Date : 16.06.2026

THE EFFECTS OF VISCOUS WALL DAMPER TYPE AND QUANTITY ON STRUCTURAL BEHAVIOR

VİSKOZ SÖNÜMLEYİCİ DUVAR TİP VE ADEDİNİN YAPISAL DAVRANIŞ ÜZERİNDEKİ ETKİLERİ

Ali Erdem ÇERÇEVİK[1] (ORCID: 0000-0002-0617-1818)

[1] Bilecik Şeyh Edebali University, Department of Civil Engineering, Faculty of Engineering, Bilecik, Türkiye

*Sorumlu Yazar / Corresponding Author: Ali Erdem ÇERÇEVİK, erdem.cercevik@bilecik.edu.tr

ABSTRACT

Energy dissipation devices, characterized by their capacity to reduce seismic demands, are widely implemented as effective and innovative solutions for the structural protection of buildings. Viscous Wall Dampers (VWD) also provide significant advantages, particularly in the design of high-rise reinforced concrete buildings and the retrofitting of existing structures without compromising architectural aesthetics. This study investigates the effectiveness of using different types and quantities of VWDs on the dynamic performance of a reinforced concrete building. Twelve models were generated based on combinations of width, wing, and quantity parameters to evaluate the performance of the VWD. A 10-story reinforced concrete building was analyzed using nonlinear time history analysis methodology under 11 scaled ground motions compliant with TBEC 2018. Parameters such as inter story drift ratio, displacement, story acceleration, story shear force, and damping were compared. Displacement and force demands of the VWDs were calculated. Furthermore, the effect of VWD type and quantity on energy balances was examined. As a result of the analyses, it was found that the increase in the number of dampers was effective in limiting inter story drifts, but supplemental damping ratios exceeding 50% led to increases in story accelerations.

Keywords: Energy dissipation devices, viscous wall dampers, seismic design, reinforced concrete structures, energy balance

ÖZET

Sismik talepleri azaltma kapasiteleriyle karakterize edilen enerji sönümleyici ekipmanlar, binaların yapısal korunması için etkili ve yenilikçi çözümler olarak yaygın bir şekilde uygulanmaktadır. Viskoz Sönümleyici Duvarlar (VWD) da, özellikle yüksek katlı betonarme binaların tasarımında ve mevcut yapıların mimari estetiği bozmadan güçlendirilmesinde önemli avantajlar sağlamaktadır. Bu çalışma, farklı tip ve miktarlarda VWD kullanımının, betonarme binaların dinamik performansı üzerindeki etkinliğini incelemektedir. VWD'lerin yapı üzerindeki etkilerini incelemek amacıyla genişlik, kanat ve miktar parametrelerinin kombinasyonlarından oluşan 12 model üretilmiştir. 10 katlı betonarme bir bina, TBDY 2018 ile uyumlu ölçeklendirilmiş 11 yer hareketi altında doğrusal olmayan zaman tanım alanında analiz metodolojisi kullanılarak analiz edilmiştir. Katlar arası öteleme oranı, yer değiştirme, kat ivmesi, kat kesme kuvveti ve sönüm gibi parametreler karşılaştırılmıştır. VWD'lerin deplasman ve kuvvet talepleri hesaplanmıştır. Ayrıca, VWD tipi ve miktarının enerji dengeleri üzerindeki etkisi incelenmiştir. Analizler sonucunda, sönümleyici sayısındaki artışın katlar arası ötelemeleri sınırlamada etkili olduğu, ancak %50'yi aşan ilave sönüm oranlarının kat ivmelerinde artışa yol açtığı belirlenmiştir.

Anahtar Kelimeler: Enerji sönümleyici ekipmanlar, viskoz sönümleyici duvarlar, sismik tasarım, betonarme yapılar, enerji dengesi

This work is licensed under a Creative Commons Attribution 4.0 International License (CC BY 4.0).

INTRODUCTION

Modern engineering aims to limit seismic and wind loads. Structural displacements are kept under control for specified performance levels. In this regard, energy-dissipating devices are presented as effective and innovative solutions (Özer, 2024; Patil et al., 2022). Viscous Wall Dampers (VWDs) demonstrate high success in reducing dynamic demands. These devices are particularly effective in limiting inter story drifts. Therefore, they are preferred in specific buildings where lateral displacement is critical. Using VWDs increases wind comfort and ensures seismic safety. However, further research is needed for the optimal design of these systems.

VWD systems provide architectural flexibility and require no maintenance. Their compact structure makes installation easy. Compared to cross braces, they allow more freedom in architectural design. The device does not contain pressure parts or sealing elements. The installation phase is quite easy and requires less reinforcement compared to other dampers. However, they can cause an increase in internal forces in the beams to which they are attached. This is considered a limitation from an engineering design perspective (Newell et al., 2011).

VWDs have been applied in more than one hundred structures worldwide. An example application is given in Figure 1, California Pacific Medical Center. This structure is a 15-story building modeled as a moment-resistant steel structure. Due to its proximity to the San Andreas Fault in California, which generates very strong earthquakes, a sensitive modeling process was required. A total of 153 VWDs were used in the structure to achieve the design objectives. The construction process of VWDs continues worldwide in this and many other specific structures with high earthquake risk (Love et al., 2012).

Figure 1. Building Constructed with VWD Installation (DIS, 2026)

The system is generally mounted on beams between two floors. It essentially consists of two main steel parts. The first part is a tank filled with liquid and is connected to the lower beam. The second part consists of steel fins and is fixed to the upper beam. Energy is dissipated by the movement of the fins within the liquid. The appearance and conceptual assembly of the Viscous Wall Dampers (VWDs) into structural elements are schematically shown in Figure 2. Energy dissipation is achieved through the additional damping provided by the VWDs to the system. This energy dissipation is provided as a result of the in-plane relative motion of the vanes inside the tank and the resulting inter-story displacement and velocity.

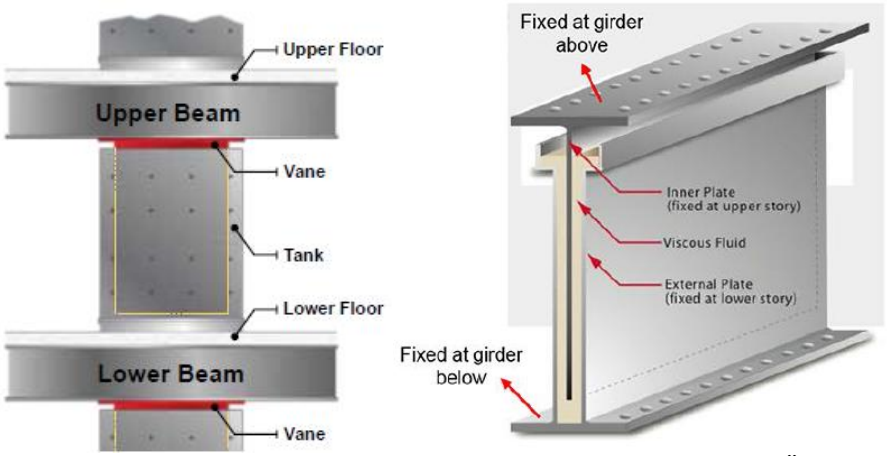

Figure 2. Schematic View of VWD Components and Concept Installation (Dilsiz & Özuygur, 2022; DIS, 2017)

Bi-directional loading tests to determine the behavior of VWDs during earthquakes were completed at the University of California. The force-displacement curves obtained from these tests are given in Figure 3a. The hysteresis curve of the force-displacement curve obtained from the tests was prepared by Newell (Newell et al., 2011). VWDs typically exhibit a higher force capacity on the first excursion to large displacements. Although the force capacity remains approximately constant in subsequent cycles, the displacement decreases. Accordingly, VWDs engage after a certain force is exceeded. This force is shown as F_0 in the hysteresis curve. After F_0 is exceeded, the displacement increases with a constant force. At the maximum displacement (d_{max}), the VWD begins its reverse movement. Thanks to this reversible-repeated movement, the energy dissipation capacity increases by the amount of area obtained. In addition, the effective stiffness (K_{eff}) occurs at the point where the maximum displacement and force are located, as shown in Figure 3b.

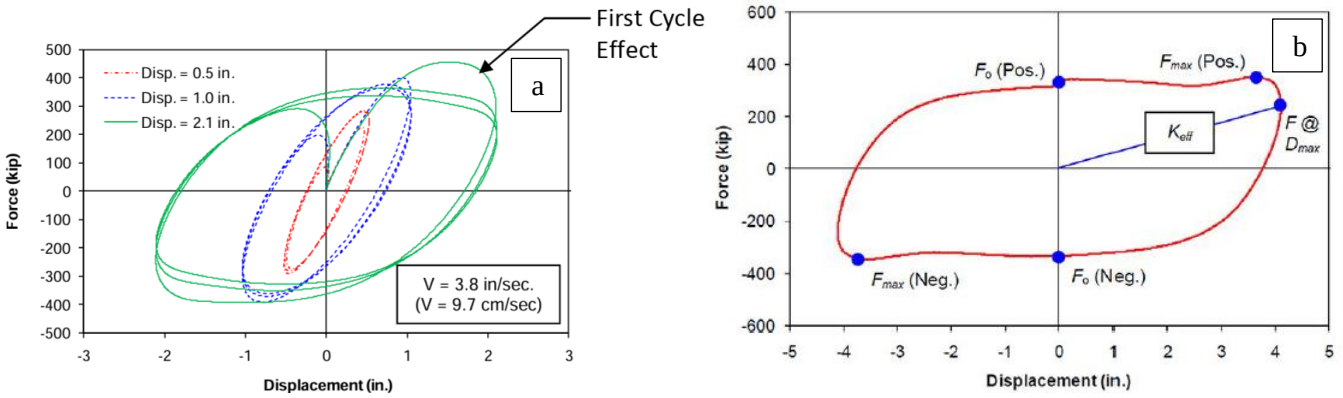

Figure 3. VWD Force-Deformation (a) and Hysteresis Curve (b) The Result of a Selected Cyclic Test (DIS, 2009; Newell et al., 2011)

Following the initial studies on VWDs in the late 1980s, VWDs have become the focus of numerous studies (Arima et al., 1988; Miyazaki et al., 1986). Lu et al. created a 3D, 3-story experimental model with viscous damping walls and tested it on a shaking table. They showed that the experimental findings coincided with the finite element program results (Lu et al., 2008). They determined that the damping ratio of the viscous damping model increased by 20% and the displacement decreased by 30% to 60%. In a similar study, a new generalized Maxwell model incorporating time-varying stiffness and damping characteristics is proposed to evaluate the seismic performance of VWDs. The accuracy of this analytical model was tested through comprehensive shaking table tests on a 1:4 scale three-story steel frame under various earthquake scenarios. The experimental results indicated that VWDs significantly increased the natural frequencies of the structure, remarkably limited displacements, and substantially reduced story accelerations and shear forces. Furthermore, dynamic simulations of the proposed model conducted via OpenSees software demonstrated high correlation with experimental data, proving the model's effectiveness and reliability in structural analysis (Zhou et al., 2018).

Hidayaty et al. conducted analyses by placing viscous damping walls in a 3-story, 3D steel frame. As a result of structural analyses performed with a combination of 3 different earthquake data, the structural period decreased while the angular frequency increased. When a 2-way viscous damping wall was placed in the model, the horizontal displacement decreased by 51%, while it decreased by 24% when a unidirectional viscous damping wall was placed (Hidayaty et al., 2018).

Dilsiz et al. conducted performance analyses of high-rise buildings with viscous damping walls in their study. They performed time-domain analyses of a 30-story reinforced concrete building using 7 earthquake acceleration records (Dilsiz et al., 2018). They compared the periods and relative story displacements of the building's models with and without viscous damping walls (VDs). They determined that viscous damping walls reduced the building's story displacements by 18-20%, and the relative displacement of the roof floor was 20% less. They calculated that relative story displacements were reduced to 1.5% in the design of a structure with viscous damping walls. Similarly, Dilsiz et al. demonstrated the advantages of VWDs on the structural behavior by considering a moment-resistant building model (Dilsiz et al., 2022). In one study, the optimum placement of VWDs in a 30-story reinforced concrete building was investigated. The study aimed to use a minimum number of VWDs by limiting relative story displacements and acceleration. Heuristic optimization algorithms were used to determine the correct spans in the structure (Çerçevik et al., 2021).

Furthermore, the use of VWDs in structures under torsional irregularity was examined. Time-history analyses were conducted on a 22-story RC structure using 5 different VWD placement combinations. It was determined that torsional irregularity could be eliminated with the optimum placement of VWDs (Dilsiz & Özuygur, 2022).

Another aspect that must be examined for passive control systems such as VWD is their energy dissipation capacity. During an earthquake, the input energy transmitted to the structure should be dissipated by the structural components. Unlike conventional structures, those equipped with passive control systems acquire additional energy dissipation capacity. The energy dissipation ratios of models with passive dampers should be carefully examined. This examination forms the basis of energy-based design. In the method based on the principle that the energy transmitted to the structures by strong ground motions is consumed in various ways, the input energy and the energy consumed must be equal (Housner, 1959). A portion of the input energy (E_i) is consumed by the structure during the earthquake as damping energy (E_ξ). The remaining energy disperses within the structure, activates the structure, and is consumed as kinetic energy (E_k). The energy consumption for elastic deformation (E_{se}) starts as soon as the movement begins. If this consumption is less than the input energy, the structure exhibits inelastic behavior and the energy balance is achieved with the consumption of hysteretic energy (E_h). This balance is seen in Equation 1 (Uang & Bertero, 1990).

$$E_i = E_\xi + E_k + E_{se} + E_h \quad (1)$$

A review of previous studies indicates that the performance of VWDs has generally focused on the distribution of identical VWD types within structures and on experimental investigations. However, the effect of VWD type on structural performance has not been investigated. This study investigates the effects of different types of VWD elements on structural performance. A 10-story building was generated, whose structural performance was deemed insufficient in terms of relative story-displacement ratios according to TBEC 2018. Six different types of VWD elements were placed in the building. In addition, the changes in performance were examined by varying the number of VWD elements. Furthermore, the energy consumption levels of VWD types and amounts were investigated. Damping ratios and force-displacement variations of VWD elements were determined through time history analyses performed with different VWD configurations. Based on the numerical results, the optimum amount and type of VWD elements were proposed. The aim of this study is to provide designers with a broad perspective on the selection of VWD type and quantity based on the results obtained.

MATERIAL AND METHOD

In this study, a 10-story reinforced concrete building was first generated. Subsequently, numerical models of the VWDs were defined. Different types of VWDs were added to the structure. Numerical results were obtained by performing time history analyses with 11 scaled acceleration records in accordance with TBDY 2018. Details are presented in the following sections.

Model of the Sample Building

The sample building model is a 3-meter-story model with 7 spans in one direction and 4 spans in the other. The numerical model was prepared in the ETABS finite element program (ETABS v22, 2025). The dimensions and views of the model are given in Figure 4. The dimensions of the beams, columns, and slabs are modeled using TBEC 2018 and TS500 (TBEC, 2018; TS 500, 2000). The strengths of concrete, steel yield, and steel tensile are 37 MPa, 420 MPa, and 500 MPa, respectively. All column, beam dimensions, and slab thickness were selected as 400x400 mm, 500x300 mm, and 150 mm, respectively. Beams and columns are modeled using frame elements, while stories are modeled as a rigid diaphragm. The structure loads are defined as 5 kN/m^2 dead and 5 kN/m^2 live load on the slab distributed uniformly over the area. In addition to the slab loads, a 3.25 kN/m wall load was modeled on the beams. A load combination was defined as 0.3 times the live loads and 1 times the dead loads in accordance with TS500, excluding the weight of the elements (beams, columns, and slabs). The effective section stiffness of column and beam members were defined 0.70EI and 0.35EI as defined in TBEC-2018, respectively.

The material behavior in the building model is assumed to be elastic. Due to the structural contribution of the VWD units, it is anticipated that the structural members will not show inelastic deformation. Additionally, a study showed that in a model equipped with energy dissipation systems, only a small portion of structural components enters the inelastic range (Özkaya & Gürbüz, 2026). Consistently, a similar approach in a different study verified that elastic modeling of the building models is adequate (Dilsiz & Özuygur, 2022).

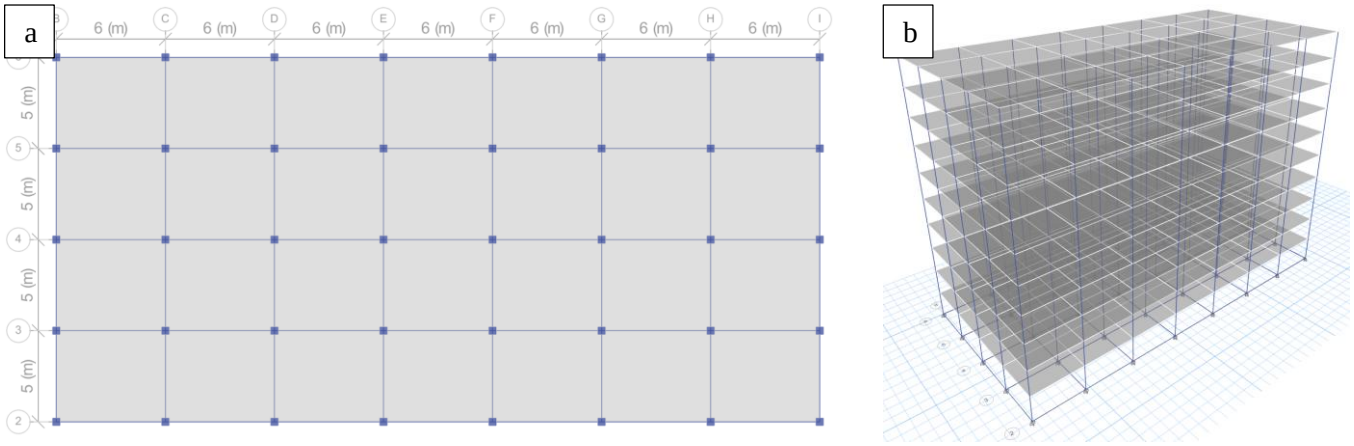

Figure 4. Non-VWD Model Views: Plan (a) and 3D View (b)

Viscous Wall Damper (VWD) Modeling

The use of energy dissipation devices such as VWDs enhances both structural and nonstructural performance under seismic excitations by reducing relative displacements and stresses in the superstructure. Given their effectiveness and cost efficiency, VWDs are recommended as a feasible solution for the design of new buildings as well as for the retrofit and strengthening of existing structures (DIS, 2017). The modeling details of VWDs were provided by the manufacturer company (DIS, 2017). The VWD modeling was done similarly to the manufacturer's catalog and previous studies (Çerçevik et al., 2021; Dilsiz et al., 2022).

According to the report prepared by the manufacturer, the modeling of the VWDs with ETABS is consistent with the experimental results. The placement of VWD equipment within the structural elements and its application in ETABS is presented in Figure 5.

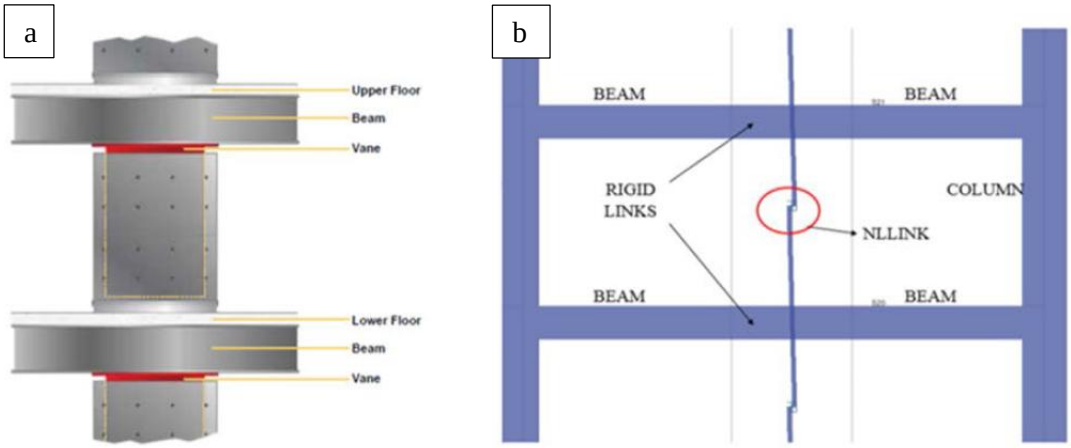

Figure 5. Placement of VWDs Between Structural Elements (a) and Their Application in ETABS (b) (DIS, 2017)

VWDs are placed between the beams along the story height as seen in Figure 5a. The ETABS model is created using an NLLINK placed between two rigid elements (Figure 5b). NLLINK elements are defined as Exponential Maxwell Dampers. In the Maxwell Damper model, the viscous damper is represented by the combination of a spring and a dashpot in series (Figure 6).

Figure 6. Schematic Representation of the Analytical Model of the VWDs (DIS, 2017)

The spring represents the stiffening property of the damper as well as its supporting member, while the dashpot represents its viscous property. The nonlinear damper force F_D is calculated as follows:

$$F_D = CV_c^{\alpha} \tag{2}$$

where C is the damper coefficient, V_c is the applied velocity, and α is the damper exponent. In addition, depending on Equation 2, three parameters must be specified in ETABS to model nonlinear VWDs: stiffness (K), damping (C), and the damping exponent (α). These parameters were previously determined by the manufacturer in accordance with Equation 2 through experimental studies. Designers can select the appropriate VWD type (DIS, 2017; page 4) for their model and implement it in ETABS; however, since both the type and quantity of VWDs directly influence structural performance, they must be chosen with particular care.

VWD Types and Layout Configurations

The layout, mechanical properties, quantity, and location of VWDs directly affect structural performance. This study investigates the performance of different VWD types provided by the manufacturer. According to the manufacturer's report, story height is the primary criterion for VWD selection; for the example model with a 3-meter-story height, six suitable VWD types were identified, consisting of combinations of width and vane configurations. The vanes are classified into two categories: single and double. In addition, the number of VWDs was varied to examine performance changes, thereby assessing both type and quantity effects. The analysis matrix for different VWD types and quantities is presented in Table 1.

Table 1. The Experimental Matrix and Parameters Prepared According to the Type and Quantity of VWDs

Model Code	Axis with VWD	Total Number of VWD	VWD Parameters					
			Width (m)/(ft)	Height (m)	Vane	K (kN/m)	C (kN(s/m)^2)	α
Non_VWD	0	0	-	-	-	-	-	-
2A_6_SV	2	40	1.83/6	3	Single	57999.12	2024	0.5
2A_7_SV	2	40	2.13/7	3	Single	70887.81	2254	0.5
2A_8_SV	2	40	2.44/8	3	Single	82165.42	2484	0.5
6A_6_SV	6	120	1.83/6	3	Single	57999.12	2024	0.5
6A_7_SV	6	120	2.13/7	3	Single	70887.81	2254	0.5
6A_8_SV	6	120	2.44/8	3	Single	82165.42	2484	0.5
2A_6_DV	2	40	1.83/6	3	Double	115998.2	4048	0.5
2A_7_DV	2	40	2.13/7	3	Double	141775.6	4508	0.5
2A_8_DV	2	40	2.44/8	3	Double	164330.8	4968	0.5
6A_6_DV	6	120	1.83/6	3	Double	115998.2	4048	0.5
6A_7_DV	6	120	2.13/7	3	Double	141775.6	4508	0.5
6A_8_DV	6	120	2.44/8	3	Double	164330.8	4968	0.5

According to Table 1, analyses were conducted for a total of 13 different configurations. For clarity and ease of presentation, each configuration was assigned a model code. The coding system was prepared in the format XA_Y_ZV, where X, Y, and Z respectively denote the number of axes containing VWDs, the VWD type based on width, and the vane type. The placement of VWDs and the dynamic analyses were conducted in a single direction. The VWD layouts include configurations with a total of 40 and 120 VWDs, as illustrated in Figure 7. In one model, VWDs were placed only along the edge axes, while in another model they were also installed within the interior axes. In this way, the study aimed to investigate the influence of VWD quantity on structural performance.

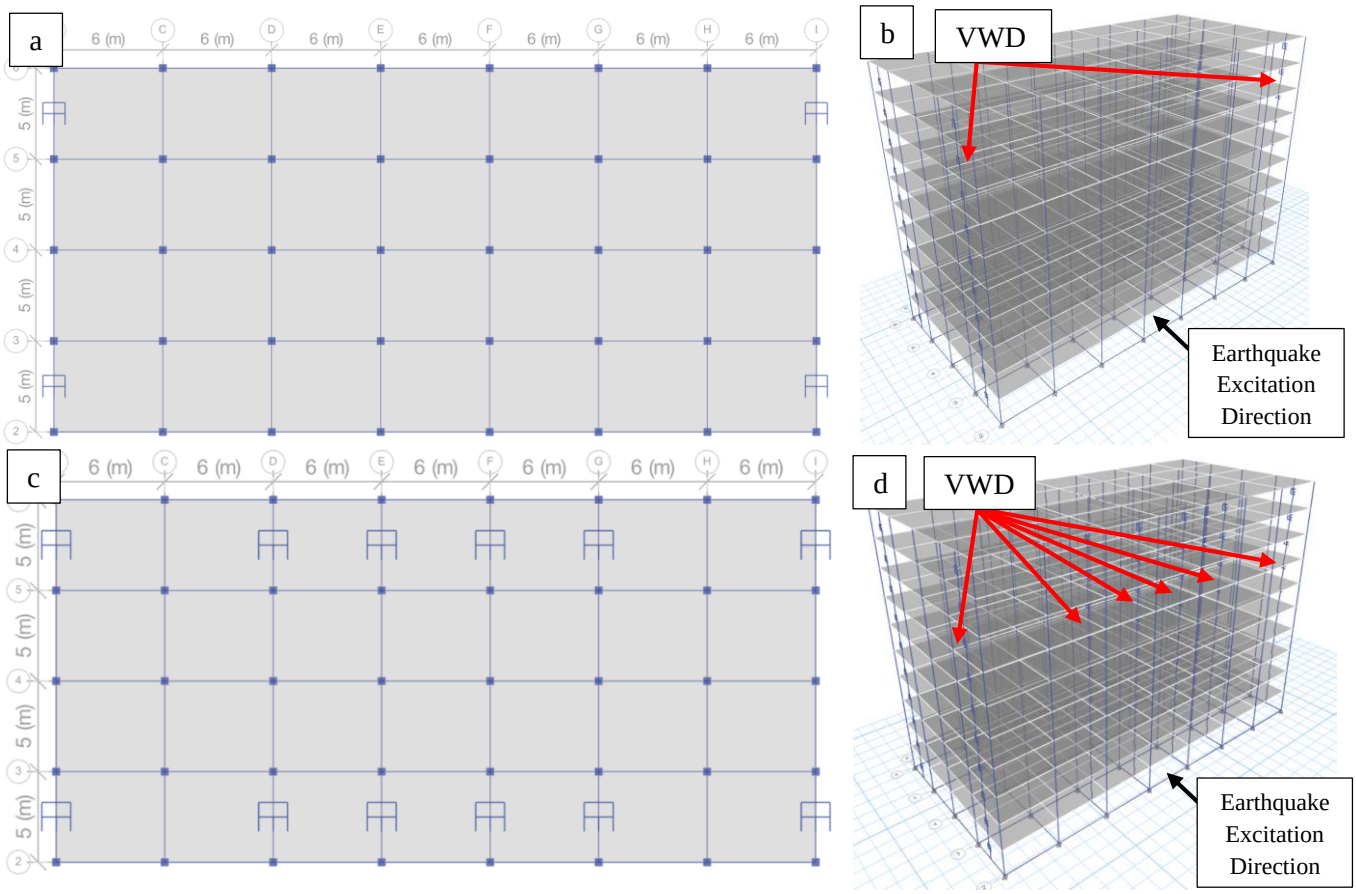

Figure 7. Plan and 3D views of the VWD Layouts for Configurations: 2-Axis Plan (a), 3D (b); 6-Axis Plan (c), 3D (d)

Ground Motions Selection

In this study, time history analyses were performed using real acceleration time series for dynamic analysis. The acceleration-time series were scaled according to TBEC 2018 (TBEC, 2018). For scaling, a design spectrum suitable for the example building was first determined. According to TBEC 2018, an elastic design spectrum was obtained according to the location of the sample models. The location of the sample model is at 41.110643° latitude and 29.086237° longitude coordinates in İstanbul province with high earthquake effects. The soil class is ZC class, which is suitable for very dense sand, gravel, and hard clay layers. The earthquake ground motion level was selected as DD1, which is a very rare earthquake ground motion where the probability of exceeding the spectral magnitudes in 50 years is 2% and the corresponding recurrence period is 2475 years. Design spectral acceleration coefficients for the sample model location, soil type and earthquake ground motion level were determined for short-period (SD_s) and 1.0 s period (SD_1) as presented in Table 2.

Table 2. Spectral Coefficients of Soil Class (ZC) and Design Earthquake Level (DD-1) for Building Location (TBEC, 2018).

Spectral Parameters	Coefficient
S_s	1.243
S_1	0.345
Short-period (SD_s)	1.492
1.0 s period (SD_1)	0.517

11 ground motion records were selected in accordance with TBEC 2018 and scaled using the simple scaling method. Since the structural analyses were performed in a single direction, the record scaling procedure was executed utilizing only a single ground motion component. In accordance with the scaling procedure, the mean of the scaled acceleration spectra shall not be less than the design spectrum within the period range of *0.2T* to *1.5T*, where *T* denotes the fundamental period of the structure. Additionally, for structures equipped with passive damping devices, the scaling must be performed considering 1.3 times the design spectrum. Figure 8 presents the design and the mean of the scaled spectra, calculated based on the fundamental vibration period of 2 seconds for the sample structure.

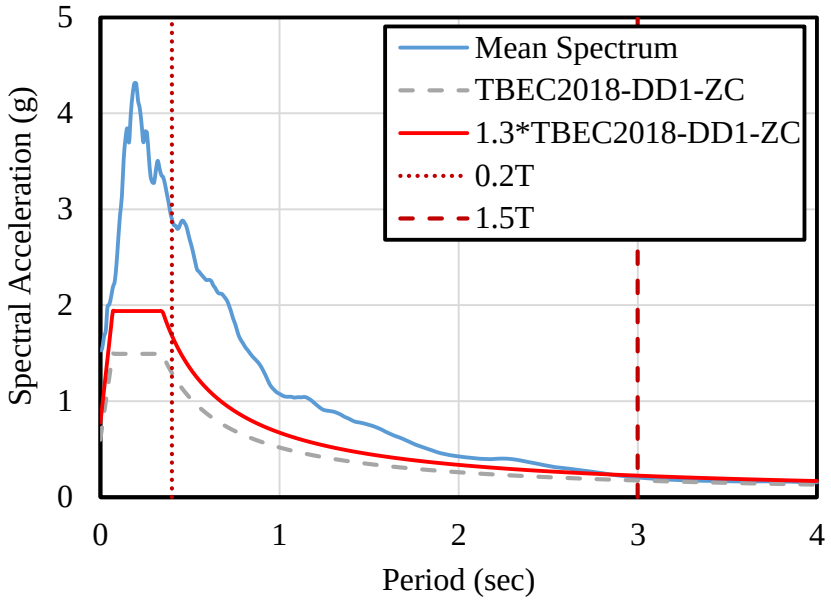

Figure 8. Elastic Acceleration Spectrum of the Scaled Records for 5% Damping (PEER, 2026; TBEC, 2018).

Although TBEC 2018 does not specify explicit criteria for ground motion selection, three different constraints were applied in this study. These criteria include a maximum distance of 25 km from the epicenter, a shear wave velocity (Vs_{30}) range of 360–760 m/s (suitable for ZC soil class), and a magnitude (M_w) between 6.5 and 7.5. The parameters of the selected ground motions and the corresponding scaling factors are presented in Table 3.

Table 3. Earthquake Ground Motions and Parameters (PEER, 2026).

RSN	Earthquake	Location	Year	M_w	Component	R_{jb} (km)	Vs_{30} (m/s)	Scale Factor
727	Superstition Hills-02	Superstition Mtn Camera	1987	6.54	B-SUP045	5.61	362.38	4
864	Landers	Joshua Tree	1992	7.28	JOS000	11.03	379.32	4
881	Landers	Morongo Valley Fire Station	1992	7.28	MVH045	17.36	396.41	3.5
1111	Kobe, Japan	Nishi-Akashi	1995	6.9	NIS000	7.08	609	3.5
1633	Manjil, Iran	Abbar	1990	7.37	L	12.55	723.95	3
1787	Hector Mine	Hector	1999	7.13	HEC000	10.35	726	4
3753	Landers	Fun Valley	1992	7.28	FVR045	25.02	388.63	4
4040	Bam, Iran	Bam	2003	6.6	L	0.05	487.4	1.5
6915	Darfield, New Zealand	Heathcote Valley Primary School	2010	7	HVSCS26W	24.36	422	3.8
8165	Duzce, Turkey	IRIGM 496	1999	7.14	496-EW	4.21	760	3.5
8166	Duzce, Turkey	IRIGM 498	1999	7.14	498-EW	3.58	425	4

Nonlinear modal time history analyses are performed using the 11 ground motions presented in Table 3. It is anticipated that VWD units will significantly reduce the deformations and damage demands on structural elements. In line with this approach, the superstructure elements are modeled with elastic material assumptions. Nonlinear modal time history analyses were deemed appropriate due to the elastic modelling of the structural frame, the inelastic modelling of the VWDs, and the significant advantages provided in terms of computational efficiency.

VWDs are defined with nonlinear material properties to more clearly determine the variations in their performance and energy dissipation capacities. This modeling strategy is preferred to represent the velocity dependent characteristics and cyclic behavior of the dampers in the most realistic manner. Thus, the damping effect of VWDs on structural responses and their mechanical efficiency are evaluated in detail.

RESULTS AND DISCUSSION

The seismic performances of the sample buildings modeled with different VWD configurations are presented in this section. The performances of the buildings were investigated based on several criteria, such as inter-story drift ratios (IDR), story accelerations, story displacements, and story shear forces. All structural performance data presented are the peak structural responses obtained during the time history analysis process. Furthermore, damping ratios were calculated using the energy component results of the buildings. In addition to the structural seismic performance, the force and displacement values of the VWDs were also examined. The most suitable configuration was determined by evaluating all the investigated seismic performance results. Initially, the IDR results for the Non-VWD structure are provided in Figure 9.

The inter story drift ratio is an important parameter in seismic performance evaluation. System performance evaluation was made according to TBEC 2018 using the calculated IDR values. In TBEC 2018, the performance limits determined according to the IDR ratio are divided into four: Uninterrupted Use (UU), Limited Damage (LD), Controlled Damage (CD), and Collapse (C), corresponding to the IDR values of 0.005, 0.01, 0.015, and >0.015, respectively (Özer & İnel, 2025; TBEC, 2018).

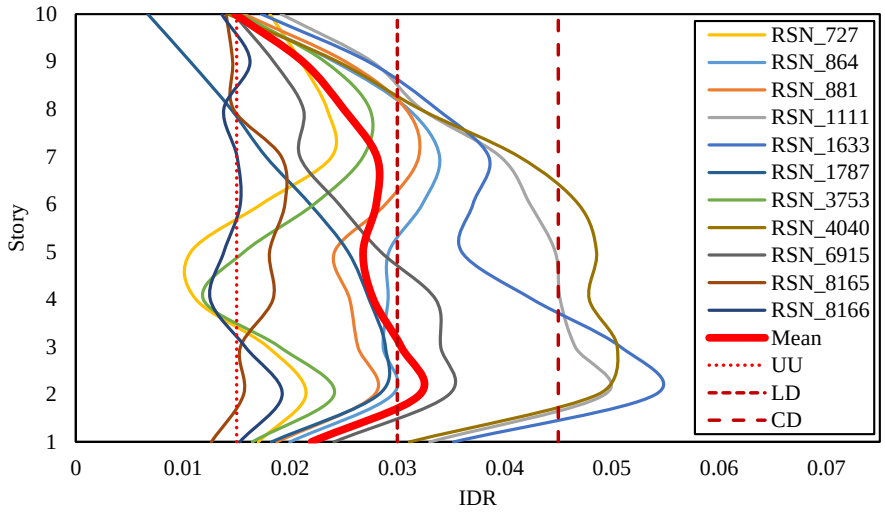

Figure 9. IDRs of the Non-VWD Building for Ground Motions

Performance limits are calculated by multiplying by the story height (3 m) in accordance with TBEC 2018. As shown in Figure 9, the maximum IDR for the non-VWD building is observed in the 1633 coded Manjil (Iran) acceleration record. Under the 1633 record, an IDR value of 0.054 is reached at the second story, exceeding the CD limit. The mean IDR exceeds the LD limit with a value of 0.03. Based on these results, the seismic performance of the non-VWD building is evaluated as insufficient.

Effect of VWD on Seismic Performance

As the main objective of the study, the configurations in Table 1 are applied to the reference building, and mean IDR values are recalculated. Mean IDR values for 11 scaled ground motions for configurations are presented in Figure 10.

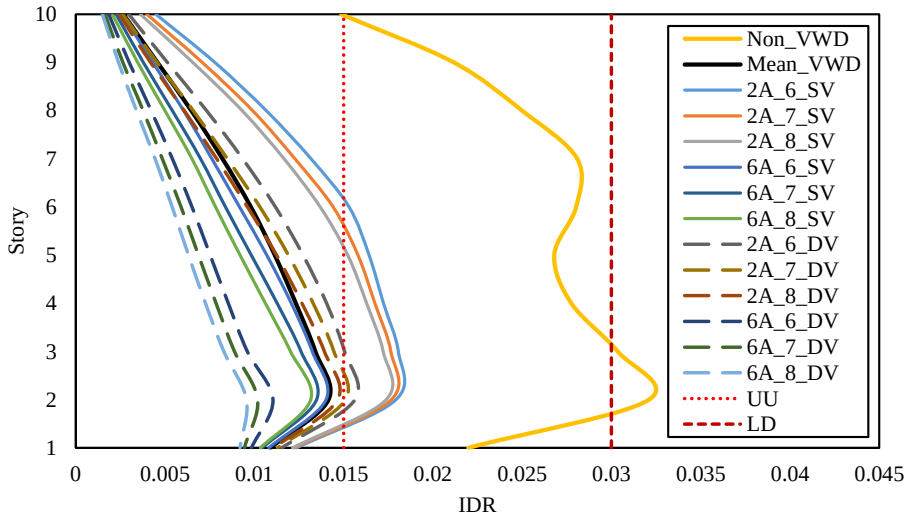

Figure 10. Mean IDRs for VWD Configurations

The mean IDRs obtained under different VWD configurations are presented comparatively in Figure 10. The analysis results clearly demonstrate the effectiveness of using VWDs in reducing structural drifts. Compared to the reference non-VWD building, a significant decrease in IDR values is observed in all models placed VWDs. It is observed that the drift ratios are gradually reduced to lower levels depending on the increase in the number of dampers.

The graphical data prove that the dampers make the drift distribution more uniform along the building height. It is determined that the UU limit is exceeded in all single-vane configurations placed on two axes (2A_6_SV, 2A_7_SV, 2A_8_SV). Among the double-vane models placed on two axes, the UU limit is also exceeded in the 2A_6_DV and

2A_7_DV configurations, with maximum IDR values of 0.0156 and 0.0151, respectively. In contrast, the 2A_8_DV configuration remains within the safe zone without exceeding the limit, with an IDR value of 0.01467.

It is observed that the UU limit is not exceeded in any of the configurations placed on six axes. In particular, it is determined that very low IDR demands occur in double-vane configurations with six-axis arrangements. These results prove that both the damper type and the quantity of placement are decisive in achieving structural performance objectives. It has been determined that an increase in the damping capacity and stiffness of VWDs does not always lead to a reduction in structural demands; furthermore, even when a reduction occurs, it may not always be economically feasible.

The maximum IDR values for 11 scaled ground motion configurations are presented in Figure 11. Unlike mean IDRs, this graph represents the most critical structural demands occurring under ground motions. It is observed that maximum IDR values in the bare structure without dampers remain at significantly high levels across all stories. With the use of VWDs, significant reductions in drift ratios are recorded even under the most unfavorable earthquake records.

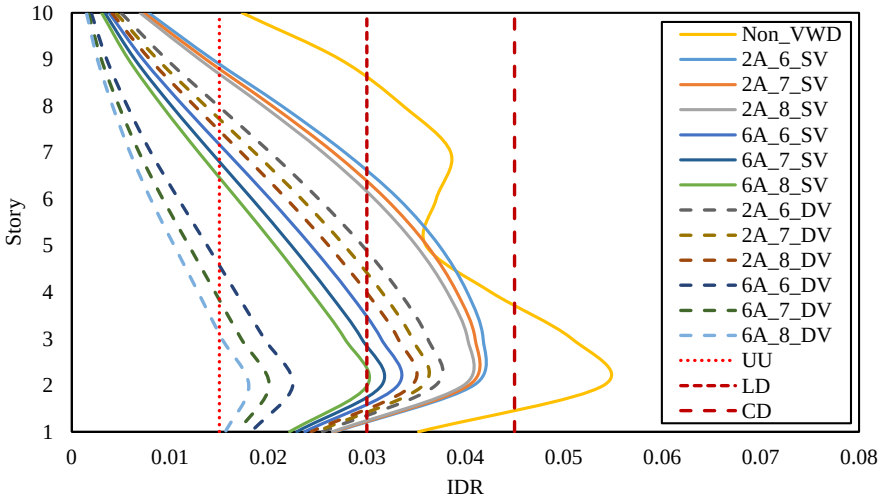

Figure 11. Maximum IDRs for VWD Configurations

The maximum IDR results presented in Figure 11 demonstrate the influence of ground motion characteristics on structural responses. For the bare building without VWDs, the highest IDR values are obtained under the 1633 coded Manjil (Iran) ground motion. In contrast, for all configurations equipped with VWDs, the maximum IDR values are recorded under the 4040 coded Bam (Iran) ground motion. This situation reveals that the dynamic characteristics of the structure change with the use of dampers. The mean story acceleration results for VWD configurations are presented in Figure 12. Story accelerations are investigated to evaluate the safety of non-structural components and comfort criteria.

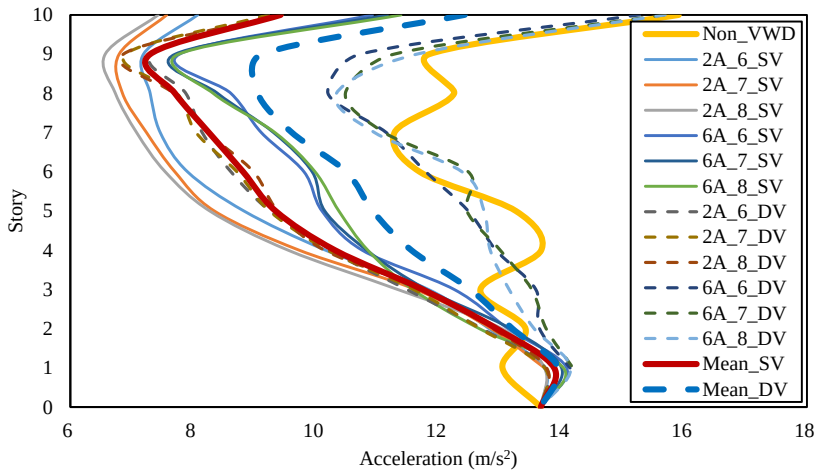

Figure 12. Mean Accelerations for VWD Configurations

According to Figure 12, the lowest mean story accelerations are observed in the single-vane configuration placed on two axes. In contrast, it is found that VWD configurations placed on 6 axes lead to higher story acceleration demands compared to those placed on 2 axes. As anticipated, the averages of the double vane configurations (Mean_DV) demand higher accelerations compared to the single vane configurations (Mean_SV). Furthermore, the double-vane configurations placed on 6 axes demand story accelerations almost identical to the non-VWD model. Based on these results, it is determined that the VWD type and quantity must be selected with great care in terms of story accelerations. The mean story displacement results for VWD configurations are presented in Figure 13.

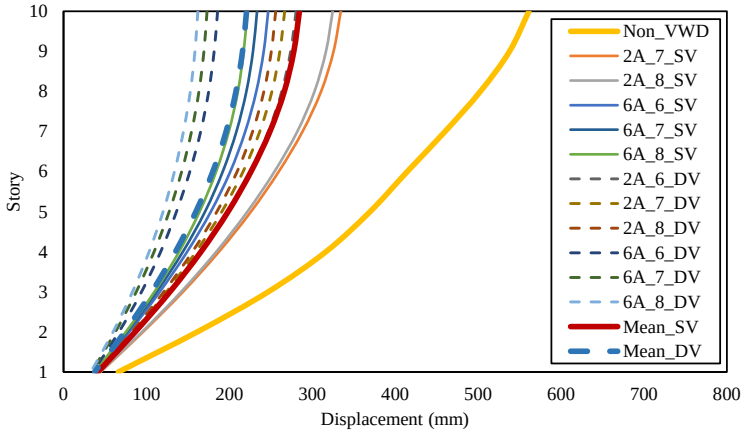

Figure 13. Mean Displacements for VWD Configurations

The story displacements are investigated to determine the overall displacement capacity of the structure under a seismic event. With the use of VWDs, it is observed that displacements at all story levels are significantly reduced compared to the non-VWD building. Notably, the reductions in displacement values at the top of the building are significant. Among the VWD-equipped structures, the peak displacement of the configuration with the highest top story demand (2A_6_SV) decreased by 39% compared to the non-VWD model, while the configuration with the lowest demand (6A_8_DV) exhibited a 71% reduction relative to the non-VWD case.

It is observed that changes in the type and amount of VWD directly affect the lateral rigidity and damping capacity of the building. The analysis results show that configurations placed on 6 axes are more successful in limiting displacements compared to those placed on 2 axes. It is determined that total displacements are reduced to the lowest levels when double-vane models are utilized.

The mean story shear force results for different configurations are presented in Figure 14. Story shear forces are investigated to determine the total lateral demand on the structural system under seismic loads. With the use of VWDs, it is observed that the shear forces concentrated in the lower stories vary at certain rates compared to the non-damped building. The energy dissipation capacity of the dampers takes over a portion of the load demand on the structural elements.

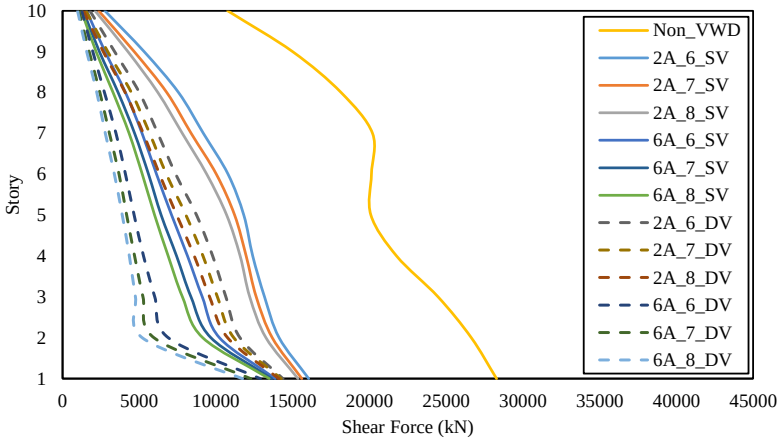

Figure 14. Mean Shear Forces for VWD Configurations

When the data presented in Figure 14 are examined, it is observed that the lowest story shear demands are calculated for configurations with VWDs placed on 6 axes. The distribution of dampers over a wider area ensures that earthquake loads are dissipated more homogeneously throughout the structure. It has been determined that the average base shear forces of VWD models decreased by 50% compared to non-VWD models. It is found that dynamic stresses on the structural system elements are significantly reduced through this arrangement.

Impact of VWD on Energy Components and Damping

This section of the study investigates the effect of VWDs on energy components. As described in Section 1, these energy components consist of input, kinetic, potential, viscous damping, and link damping elements. The energy dissipation components obtained from the seismic analyses are presented in Figure 15.

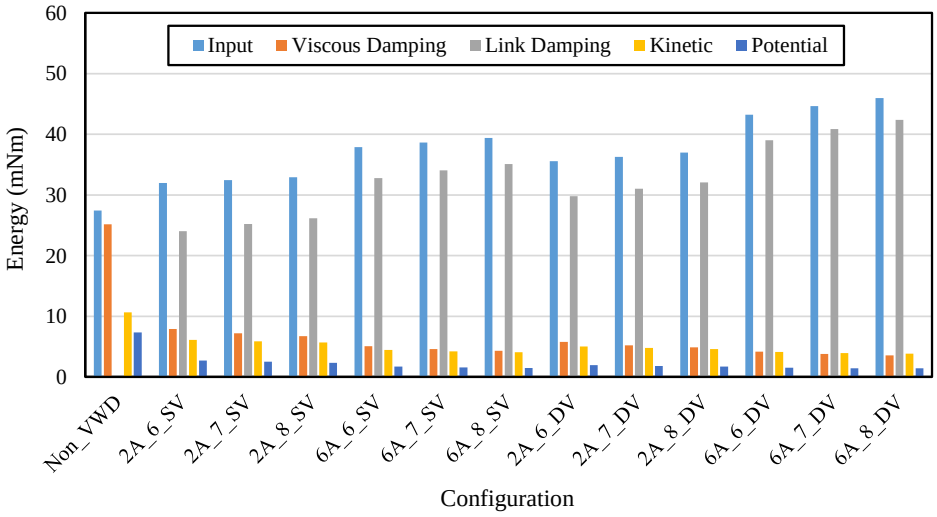

Figure 15. Energy Components for VWD Configurations

As shown in Figure 15, the lowest input energy is calculated in the structure without VWD, while the highest viscous damping is also calculated in the structure without VWD. This result indicates that the high link dissipation energy generated in structures with VWD increases the input energy. However, it has been calculated that the viscous damping energy, which can cause structural damage, is approximately four times higher in buildings without VWD compared to buildings with VWD. Furthermore, it is observed that the double-vane type has a higher damping capacity for link damping energy compared to the single-vane type. Although the link damping energy increases as expected with increasing VWD amount, it has been determined that the increase is not linear.

In this study, the damping ratios of the configurations were also calculated using energy components. The damping ratio is calculated based on the relationship between viscous damping energy, link damping energy, and structural damping values. The damping ratio, derived from energy components, is calculated by multiplying the structural damping ratio by the ratio of link damping energy to the total viscous damping energy (Taylor Devices, 2025; Zhou et al., 2022). Since the sample model is a reinforced concrete structure, a structural damping of 5% can be accepted. With this calculation method, the supplemental damping capacity provided to the system by the dampers is numerically determined (Figure 16).

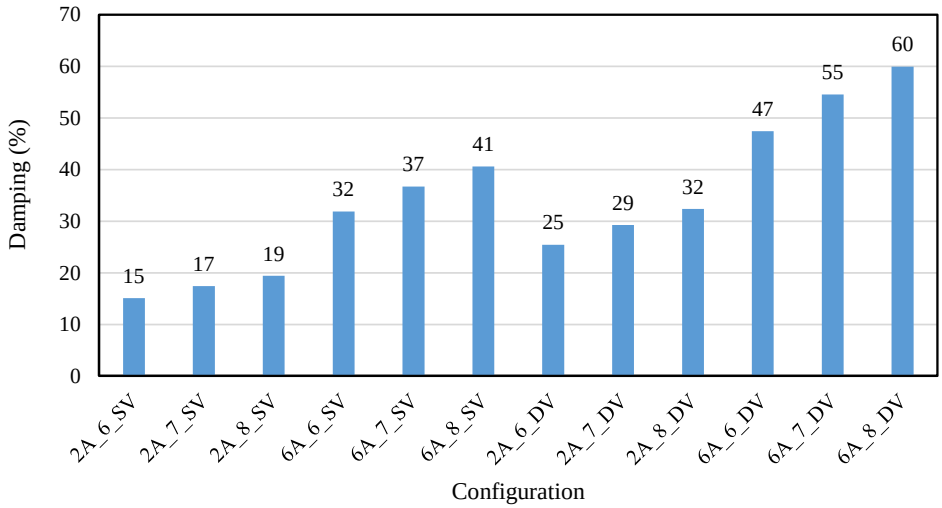

Figure 16. Damping Ratios for Different VWD Configurations

The data presented in Figure 16 demonstrate the impact of damper type and placement quantity on the total damping ratio. It is observed that the effective damping ratio of the structure increases significantly depending on the increase in the number of dampers. In particular, higher damping values are achieved in double-vane configurations due to the increased energy dissipation capacity. These results verify the efficiency of VWD systems in damping the dynamic responses of the building on an energy basis.

The additional damping provided by passive energy dampers should be carefully examined. In particular, high additional damping of 50% and above both makes the results unrealistic and leads to increases in story accelerations. Figure 16 shows that the highest damping ratios were calculated in models with double vanes placed on 6 axes. The configurations in which the highest calculated story accelerations are presented in Figure 12 are also the same. These results are consistent with previous studies focusing on passive energy dissipation systems such as seismic isolation (Çerçevik et al., 2020) and fluid viscous dampers (Zhou et al., 2022).

Maximum VWD Force-Displacement Relationships

In passive energy dissipation systems, in addition to structural performance, the forces acting on the damping devices and the resulting displacements are also investigated. Even if structural performances and damping ratios are optimized by the designer, each passive energy dissipation device has specific mechanical capacities. To ensure device safety, it is determined that the maximum demands obtained from seismic analyses remain within these capacity limits. The results for the VWDs demanding the highest displacements and forces in each configuration analyzed in the study are presented in Figure 17.

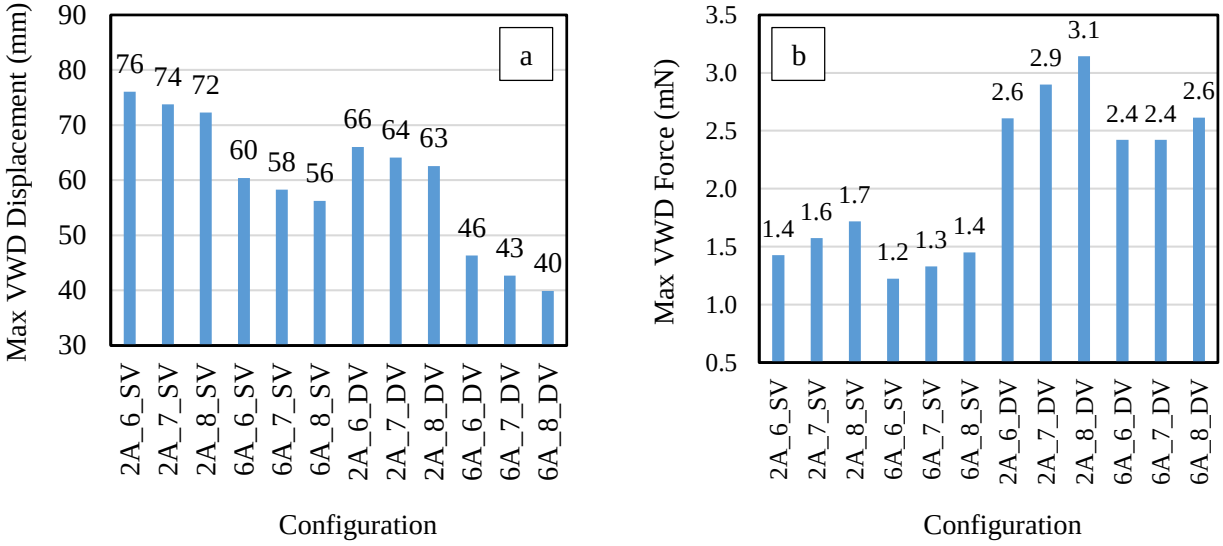

Figure 17. Maximum VWD Displacements (a), Force (b) for Different Configurations

When Figure 17 (a) is examined, it is determined that the displacement demands per device in configurations placed on 2 axes are higher than in 6-axis arrangements. This is due to the fact that the seismic displacement demands have to be met by a smaller number of units. As expected, higher displacement demands were calculated in double vane configurations compared to single vane configurations. According to the maximum force results presented in Figure 17 (b), the highest value is observed in the 2A_8_DV configuration. Furthermore, higher force values were calculated in double vane configurations. These results suggest that the structural performance advantage provided by models with double vane configurations is due to their higher force values. Figure 18 shows examples of force-displacement curves for the 2A_8_DV configuration at ground motions of 1111 and 727.

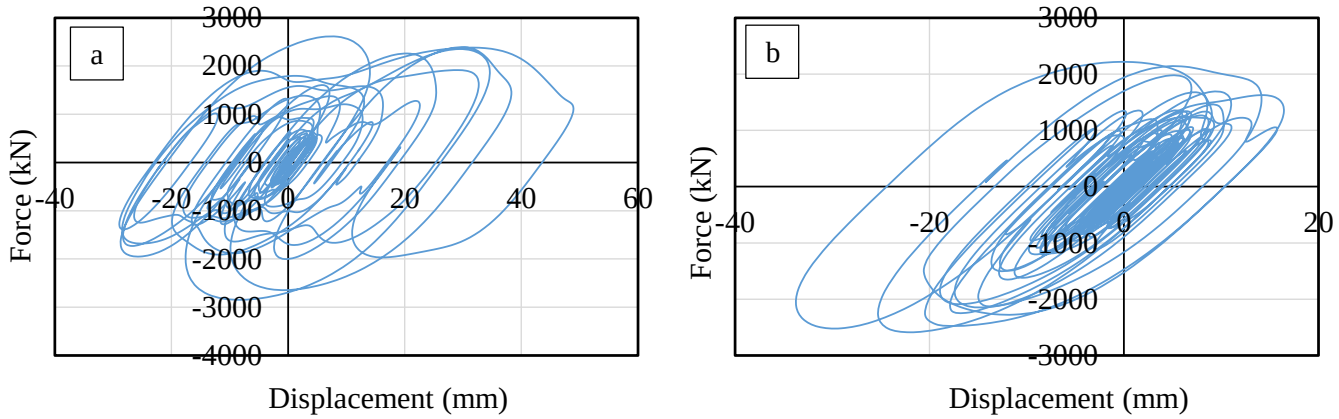

Figure 18. Force-Displacement Curves for 1111 (a) and 727 (b) Ground Motions under 2A_8_DV Configuration

Examining the force-displacement curves in Figure 18, it can be seen that the modeled VWD elements, like other passive energy-dissipating devices, add extra damping to the structure by performing numerous cycles. The stable form exhibited by the hysteresis curves reveals that the dampers maintain their energy dissipation function without performance loss under repeated loadings. The two sample force-displacement curves obtained were found to be consistent with the typical curves given in Figure 2 and with the experimental results obtained in a previous study (DIS, 2026). The size of the area enclosed by the curves confirms the mechanical efficiency of the dampers and their capacity to meet seismic demands.

CONCLUSION

This study evaluates the effectiveness of diverse VWD configurations and quantities on the dynamic performance of a high rise RC building under seismic loads. To examine the effectiveness of the VWD type, six different configurations were generated with variable width and vane type. Initially, VWDs were placed on two axes of the sample model. Subsequently, the number of axes with VWDs was increased from two to six, and the total number of VWDs was increased from 40 to 120. This aimed to examine the effects of changes in VWD quantities on structural performance. Analyses were performed on 13 different models: a reference model without VWDs, and configurations with VWDs placed on two and six axes.

Nonlinear modal time history analyses were performed on a 10-story RC building located in Istanbul, using 11 scaled ground motions in accordance with TBEC 2018. As a result of the analyses, structural performance was examined in terms of IDR, story displacements, accelerations, and shear forces. Furthermore, the effect of changes in VWD type and quantity on energy components was investigated. The additional damping provided by VWDs was examined using energy components.

The obtained results are presented in the items below:

- With the use of VWDs, significant reductions in IDR and total story displacements were recorded in all configurations.
- It is observed that increasing the damper quantity is effective in limiting IDRs but may lead to increases in story accelerations. In particular, in 6-axis double-vane configurations with supplemental damping ratios exceeding

50%, acceleration demands reached the levels of the non-VWD model. Considering that seismic codes limit the supplemental damping ratio provided by energy dissipation devices to 30%, the fact that certain configurations yield damping ratios around 50% clearly demonstrates that damping properties must be rigorously controlled and monitored by structural designers.

- The fact that maximum IDR results were obtained under different ground motions (Manjil and Bam) reveals the critical importance of ground motion selection and the use of multiple records in VWD design.
- It was determined that the force-displacement characteristics of the VWD units were consistent with experimental data in the literature. It was determined that the physical capabilities of VWD equipment should be carefully considered in VWD design.
- According to the numerical results, the optimum configuration was evaluated as 2A_8_DV. This evaluation was made at 3 points as follows: Configurations whose average IDR values exceeded the UU limit (2A_6_SV, 2A_7_SV, 2A_8_SV, 2A_6_DV, 2A_7_DV) were eliminated. Configurations with 6-axis double vane (6A_6_DV, 6A_7_DV, 6A_8_DV) with similar floor acceleration calculations to the Non-VWD model were eliminated. Single vane configurations with 6 axes (6A_6_SV, 6A_7_SV, 6A_8_SV) were also eliminated because, despite having a higher amount of VWD compared to 2A_8_DV, their positive contribution to structural performance was lower. The optimum configuration was selected as 2A_8_DV, but this is also the configuration with the highest force value. Since the manufacturer did not limit the maximum force values, 2A_8_DV was considered the optimum configuration.

According to all the results obtained, for buildings equipped with VWD, the selection of ground motion, building responses, damping ratio, and the physical capacities of the VWDs must be carefully considered. Determining the optimum VWD type and quantity using meta-heuristic algorithms, considering all parameters addressed in the study, is among the future works.

Artificial Intelligence Contribution Statement

This manuscript was entirely written, edited, analyzed, and prepared without the assistance of any artificial intelligence tools. All content, including text, data analysis, and figures, was solely generated by the authors.

REFERENCES

Arima, F., Miyasaki, M., Tanaka, H., & Yamasaki, Y. (1988). A study on building with large damping using viscous damping walls. *Ninth World Conference on Earthquake Engineering*, 821–826.

Çerçevik, A. E., Avşar, Ö., & Dilsiz, A. (2021). Optimal placement of viscous wall dampers in RC moment resisting frames using metaheuristic search methods. *Engineering Structures, 249*, 113108. https://doi.org/10.1016/j.engstruct.2021.113108

Çerçevik, A. E., Avşar, Ö., & Hasançebi, O. (2020). Optimum design of seismic isolation systems using metaheuristic search methods. *Soil Dynamics and Earthquake Engineering, 131*(106012). https://doi.org/10.1016/j.soildyn.2019.106012

Dilsiz, A., Mohammed, M. S., Özuygur, A. R., Moustafa, M. A. (2018). Evaluation of Wall Damper Effectiveness on the Seismic Performance of High-Rise Buildings. *11th National Conference on Earthquake Engineering*, 25–29.

Dilsiz, A., Mohammed, M. S., Moustafa, M. A., & Özuygur, A. R. (2022). Seismic Design and Performance of Reinforced Concrete Special Moment Resisting Frames with Wall Dampers. *Journal of Earthquake Engineering*, *26*(2), 744–763. https://doi.org/10.1080/13632469.2019.1692741

Dilsiz, A., & Özuygur, A. R. (2022). Suppression of the torsional irregularity of high-rise buildings using viscous wall dampers. *Bulletin of Earthquake Engineering*, *20*(8), 4237–4257. https://doi.org/10.1007/s10518-022-01371-6

DIS. (2009). *Viscous Wall Dampers: Superior Earthquake Protection for Flexible Buildings*. Dynamic Isolation Systems. https://www.dis-inc.com/pdf_files/DIS_VWD.pdf

DIS. (2017). *Dynamic Isolation Systems Inc. (DIS), McCarran, NV*. Viscous Wall Dampers: Guidelines for Modeling. https://www.dis-inc.com/pdf_files/DIS Viscous Wall Dampers - Guidelines for Modeling.pdf

DIS. (2026). *Viscous Wall Damper Modeling Guide*. www.dis-inc.com

ETABS v22. (2025). *Integrated Building Design Software, Computers and Structures, Inc: Berkeley, California.* (V22.6.0). https://www.csiamerica.com/products/etabs

Hidayaty, E., Setio, H. D., Surahman, A., & Moestopo, M. (2018). Numerical Analysis of Viscous Wall Dampers on Steel Frame. *MATEC Web of Conferences*. https://doi.org/10.1051/matecconf/201814701001

Housner, G. W. (1959). Behavior of structures during earthquakes. *Journal of the Engineering Mechanics Division*, *85*(4).

Love, R., Newell, J., Sinclaire, M., Chen, Y., & Poland, C. (2012). Performance-Based Design of an Essential Hospital with Supplemental Viscous Damping in a High Seismic Zone. *15th World Conference on Earthquake Engineering (15WCEE).*

Lu, X., Zhou, Y., & Yan, F. (2008). Shaking Table Test and Numerical Analysis of RC Frames with Viscous Wall Dampers. *Journal of Structural Engineering*, *134*(1), 64–76. https://doi.org/10.1061/(asce)0733-9445(2008)134:1(64)

Miyazaki, M., Arima, F., Kidata, Y., & Hristov, I. (1986). Earthquake response control design of buildings using viscous damping walls. *Proc. of 1st East Asian Conf. on Structural Eng. and Construction*, 1882–1891.

Newell, J., Love, J., Sinclair, M., Chen, Y. N., & Kasalanati, A. (2011). Seismic design of a 15 story hospital using viscous wall dampers. *Structures Congress 2011 - Proceedings of the 2011 Structures Congress*, 815–826. https://doi.org/10.1061/41171(401)72

Özer, E. (2024). The effect on required gap distance in adjacent reinforced concrete buildings of fluid viscous dampers. *Niğde Ömer Halisdemir University Journal of Engineering Sciences*, *13*(4), 1231–1239. https://doi.org/10.28948/ngumuh.1499280

Özer, E., & İnel, M. (2025). The effect of single and combined use of base isolator and fluid viscous damper on seismic performance in a conventional RC building with torsional irregularity. *Journal of Building Engineering*, *101*, 111898. https://doi.org/10.1016/j.jobe.2025.111898

Özkaya, Ö. F., & Gürbüz, M. (2026). Efficacy of fluid viscous damper placement strategies on the seismic response of an irregular high-rise composite building. *Bulletin of Earthquake Engineering*, *24*, 4377–4407. https://doi.org/10.1007/s10518-026-02428-6

Patil, B. I., Biradar, B. B., & Doddamani, R. (2022). Mitigation of Seismic Pounding Observed in Adjacent Buildings with Fluid Viscous Damper. *Lecture Notes in Civil Engineering*, *162*, 711–731. https://doi.org/10.1007/978-981-16-2826-9_45

PEER. (2026). *Ground Motion Database*. Shallow Crustal Earthquakes in Active Tectonic Regimes, NGA-West2. http://ngawest2.berkeley.edu/

Taylor Devices. (2025). *Fluid Viscous Dampers General Guidelines for Engineers Including a Brief History*. https://www.taylordevices.com/products/fluid-viscous-damper/#Brochures

TBEC. (2018). *Turkish Building Earthquake Code, Principles for the design of buildings under earthquake*.

TS 500. (2000). *Design and Construction Rules of Concrete Turkish Standards Institute*.

Uang, C. -M, & Bertero, V. V. (1990). Evaluation of seismic energy in structures. *Earthquake Engineering & Structural Dynamics*. https://doi.org/10.1002/eqe.4290190108

Zhou, Y., Chen, P., Zhang, D., Gong, S., & Lu, W. (2018). A new analytical model for viscous wall dampers and its experimental validation. *Engineering Structures*, *163*, 224–240. https://doi.org/10.1016/j.engstruct.2018.02.049

Zhou, Y., Sebaq, M. S., & Xiao, Y. (2022). Energy dissipation demand and distribution for multi-story buildings with fluid viscous dampers. *Engineering Structures*, *253*, 113813. https://doi.org/10.1016/j.engstruct.2021.113813